nature cell biology

DOI: 10.1038/ncb2324

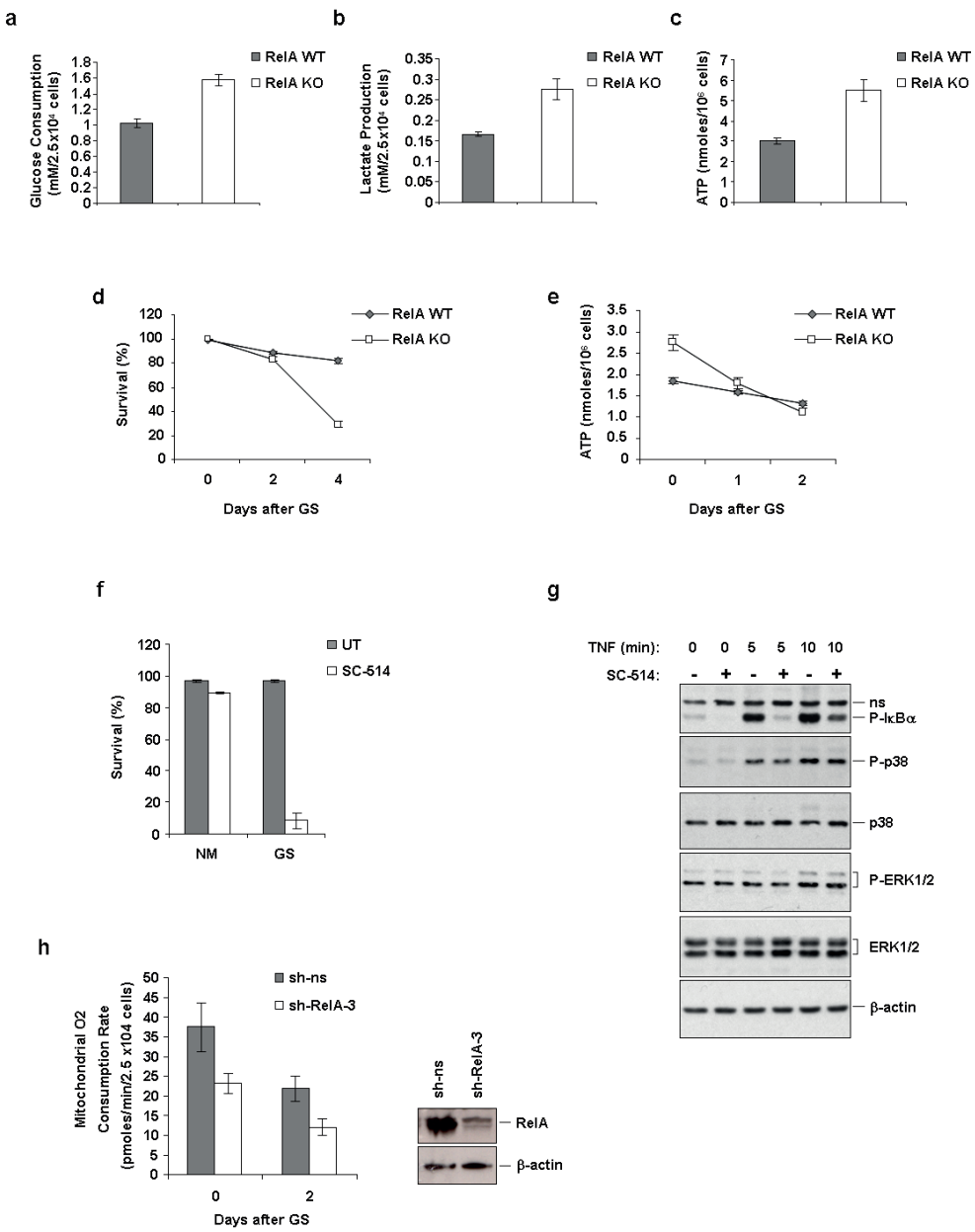

Figure S1 NF-κB counters aerobic glycolysis and promotes adaptation to GS in MEFs. (**a-c**) Glucose consumption, lactate production and intracellular ATP concentration in early-passage *RelA*$^{-/-}$ (KO) and *RelA*$^{+/+}$ (WT) MEFs, under normal culture conditions. Similar results were obtained using two additional clones of mutant and wild-type MEFs. (**d**) Viability of early-passage *RelA*$^{-/-}$ and *RelA*$^{+/+}$ MEFs after GS. (**e**) Intracellular ATP concentration in MEFs treated as in (**d**). Lactate concentration for either *RelA*$^{-/-}$ or *RelA*$^{+/+}$ MEFs could not be determined following complete glucose withdrawal because they were below the detection limit of the assay. (**f**) Viability of immortalized MEFs after a 3-day culture in normal medium (NM) or medium containing 6 mM glucose (GS), either in the presence (SC-514) or absence (UT) of the IKKβ inhibitor, SC-514 (20 μM). (**g**) Western blots showing phosphorylated (P) IκBα, and total and phosphorylated p38 and ERK in immortalized MEFs, either left untreated or treated with TNFα, in the presence (+) or absence (-) of SC-514 (100 μM). P-IκBα shows the efficacy of NF-κB inhibition, whereas P-p38 and P-ERK1/2 show the specificity of this inhibition. β-actin is shown as loading control. ns, non-specific. (**h**) Oxygen consumption in immortalized MEFs expressing sh-RelA-3 (a different RelA-specific hairpin from that used in Figs. 1d and 1g) or sh-ns sh-RNAs under normal culture conditions and during GS (left). Western blots with the same cells showing RelA knockdown efficiency and specificity (right). (**a-f**, **h**) Values denote mean ± s.e.m. (**a-f**) n=3; (**h**) n=12.

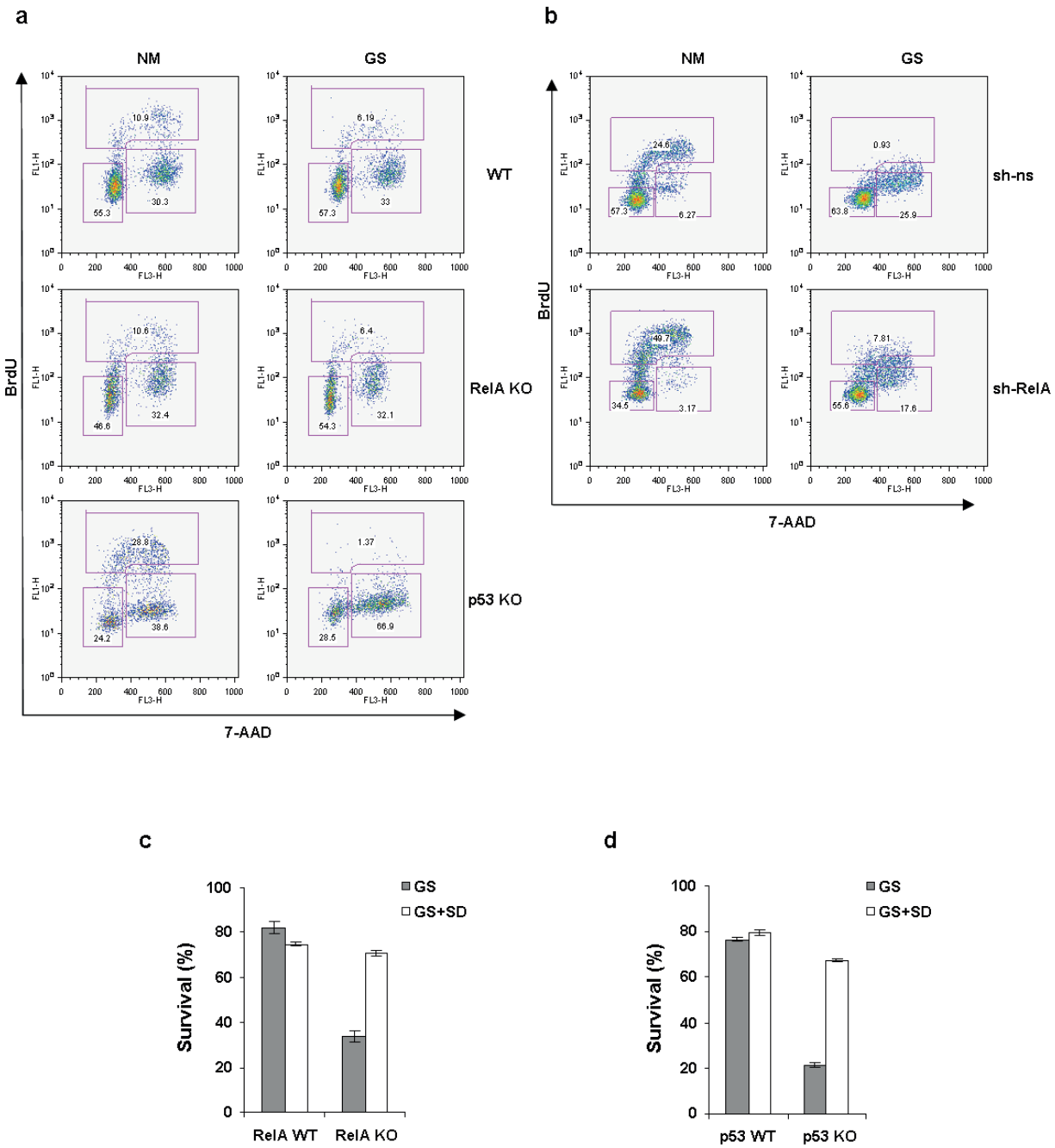

Figure S2 NF-κB or p53 deficiency does not impair cell-cycle arrest following GS, and the cytotoxic effects of this deficiency during GS are blocked by serum deprivation. (**a**) FACS analyses of early-passage *RelA*$^{-/-}$, *p53*$^{-/-}$ and wild-type (WT) MEFs cultured in normal medium (NM) or in medium containing no glucose (GS) for 48 hours, then labelled with 7-AAD and BrdU. (**b**) FACS analyses of immortalized MEFs expressing sh-ns or RelA-specific sh-RNAs cultured either in NM or in medium containing 6 mM glucose (GS) for 48 hours, then labelled as in (**a**). (**a-b**) Depicted in the dot plots are the percentages of cells in the different phases of the cell cycle (G_1, bottom, left; S, top; G_2/M, bottom, right). FL1-H, BrdU staining; FL3-H, 7-AAD staining. (**c-d**) Survival of early-passage *RelA*$^{-/-}$ (**c**), *p53*$^{-/-}$ (**d**), and wild-type MEFs after GS, either alone (GS) or in combination with serum deprivation (GS+SD) for 96 hours. (**c-d**) Values denote mean ± s.e.m. (n=3).

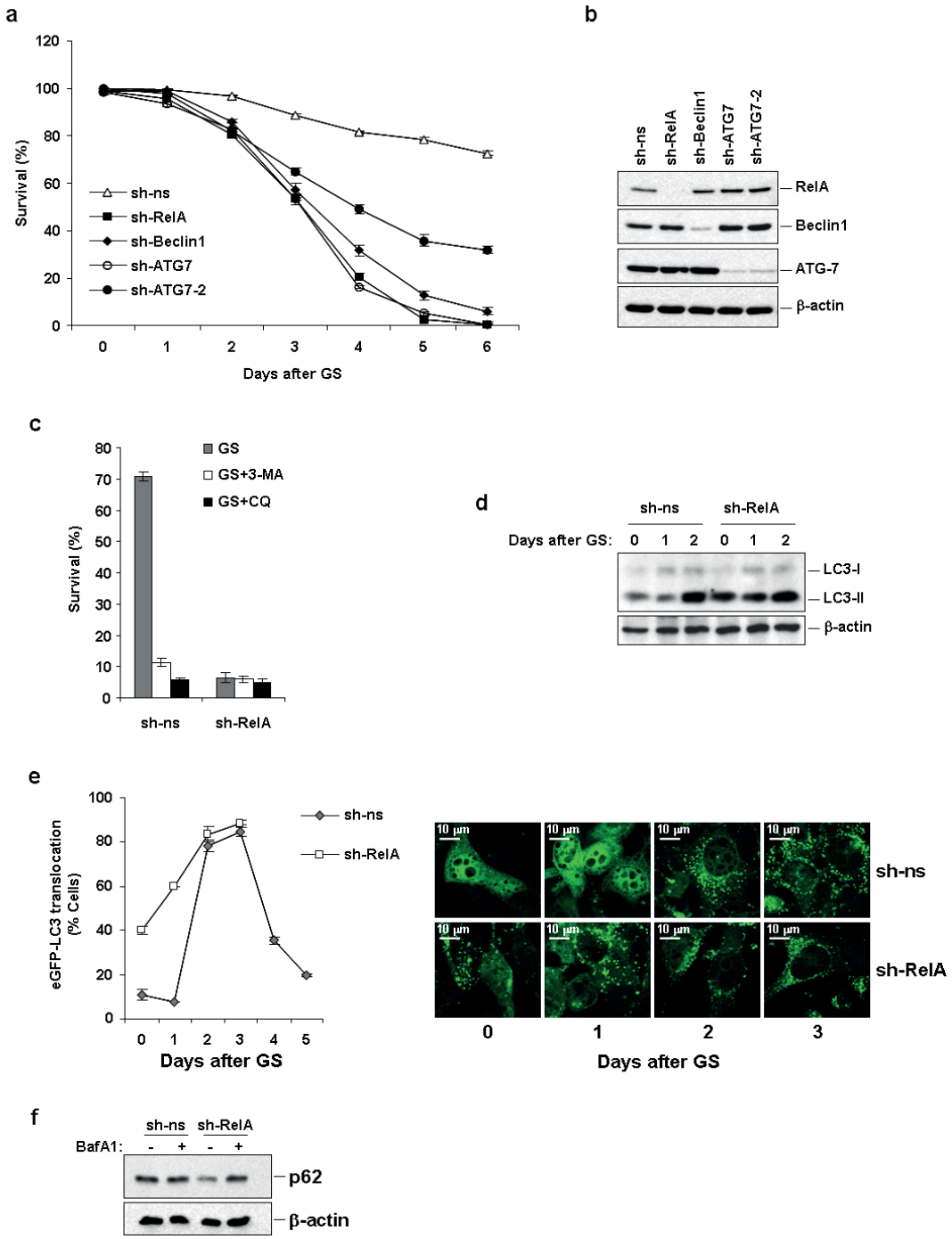

Figure S3 NF-κB does not impair the induction of macroautophagy by GS. (**a**) Survival of immortalized MEFs expressing sh-ns, sh-RelA, sh-Beclin1, sh-ATG7, and sh-ATG7-2 sh-RNAs during GS. (**b**) Western blots with antibodies against RelA, Beclin1 or ATG7 and extracts from the untreated cells shown in (**a**) (0-hour time point). (**c**) Survival of sh-ns- and sh-RelA-expressing immortalized MEFs after GS for 120 hours, either alone (GS) or in combination with 3-methyladenine (GS+3-MA) or chloroquine (GS+CQ) treatment. (**d**) Western blots showing the upregulation of LC3 in immortalized MEFs expressing sh-ns or RelA-specific sh-RNAs before and after GS. (**e**) Percentages of immortalized sh-RelA and sh-ns MEFs expressing a eGFP-fusion protein of LC3 (labelling macroautophagic vesicles[10,38]) and displaying punctuate intracellular fluorescence, before and after GS (left). The analysis of sh-RelA cells was stopped at day 3, due to massive cell death beyond this time. Representative images of the same cells (right). Of note, whilst normally supporting macroautophagy induction by GS, RelA-deficient cells displayed increased autophagosome formation under basal conditions (*see* the 0-hour time points; *see* also the increased basal protein expression of LC3 in sh-RelA cells (**d**)). (**f**) Western blots showing the levels of the autophagic cargo protein, p62, in immortalized sh-ns and sh-RelA MEFs before (-) and after (+) treatment with the lysosomal vacuolar ATPase inhibitor, bafilomycin A1. The data show that p62 levels are reduced in RelA-deficient cells under basal conditions compared to control cells, consistent with an enhanced rate of autophagosome degradation in sh-RelA cells. Accordingly, blocking this degradation with bafilomycin A1 increased p62 levels in RelA-deficient cells. Together with the data shown in (**d**) and (**e**), these results demonstrate that RelA inhibition causes an increase in basal autophagic flux, possibly owing to an enhancement of protein/organelle turnover[10]. (**b**, **d**, **f**) β-actin is shown as loading control. (**a**, **c**, **e**) Values denote mean ± s.e.m. (n=3).

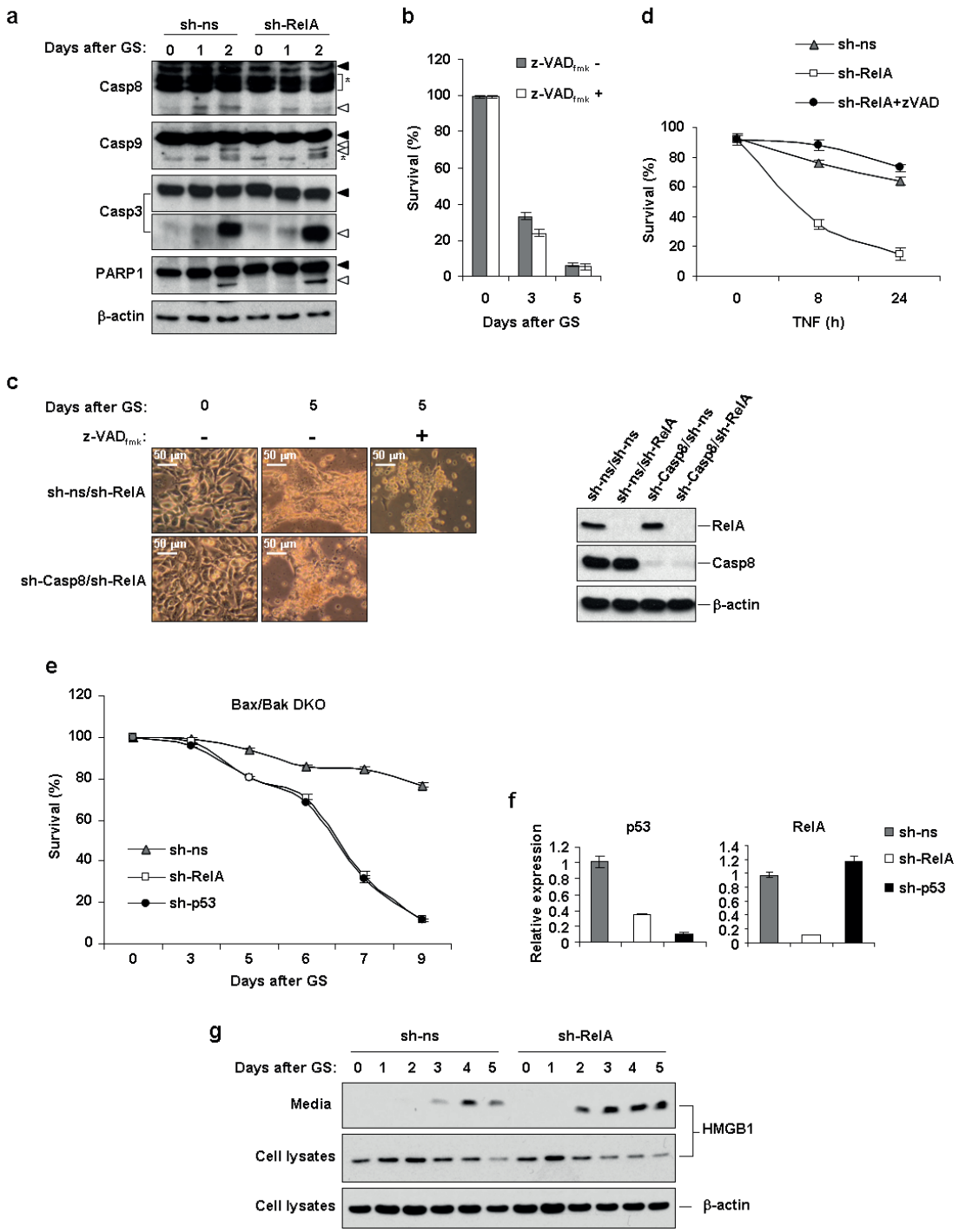

Figure S4 NF-κB-afforded protection against GS-induced killing depends on the suppression of a necrosis-like pathway of cell death. (**a**) Western blots showing the processing of Caspase-8, Caspase-9, and Caspase-3, and the cleavage of the Caspase-3 substrate, PARP1, after GS in immortalized MEFs expressing either sh-ns or RelA-specific sh-RNAs. Filled arrowheads, unprocessed proteins; open arrowheads, specific cleavage products; asterisks, non-specific bands. (**b**) Survival of immortalized sh-RelA MEFs after GS, in the presence (z-VAD$_{fmk}$ +) or absence (z-VAD$_{fmk}$ -) of z-VAD$_{fmk}$. (**c**) Images of representative cultures from (**b**) (*i.e.* z-VAD$_{fmk}$ +, day 5) and immortalized sh-RelA MEFs expressing either sh-ns (sh-ns/sh-RelA) or Casapse-8-specific sh-RNAs (sh-Casp8/sh-RelA) after GS (left). Western blots showing the expression of RelA and Caspase-8 in the same cells (0-hour time points; right). (**d**) Survival of immortalized sh-ns and sh-RelA MEFs after treatment with TNFα plus cycloheximide (CHX; 0.1 μg/ml), in the presence or absence of z-VAD$_{fmk}$, at the same concentration used in (**b**) and (**c**). These data demonstrate that RelA-deficient cells can be rescued by z-VAD$_{fmk}$ under conditions in which they are known to succumb to apoptosis[34]. (**e**) Survival of immortalized *Bax*$^{-/-}$/*Bak*$^{-/-}$ (DKO) MEFs expressing sh-ns, sh-RelA, or sh-p53 sh-RNAs before and after GS. (**f**) qRT-PCR showing the relative expression of *RelA* and *p53* in the cells in (**e**). (**g**) NF-κB inhibits the GS-induced extracellular release of the specific necrosis marker, HMGB1. Shown are Western blots with anti-HMGB1 antibody and culture media or total lysates from immortalized sh-ns and sh-RelA MEFs after GS. (**a**, **c**, **g**) β-actin is shown as loading control. (**b**, **d-f**) Values denote mean ± s.e.m. (n=3).

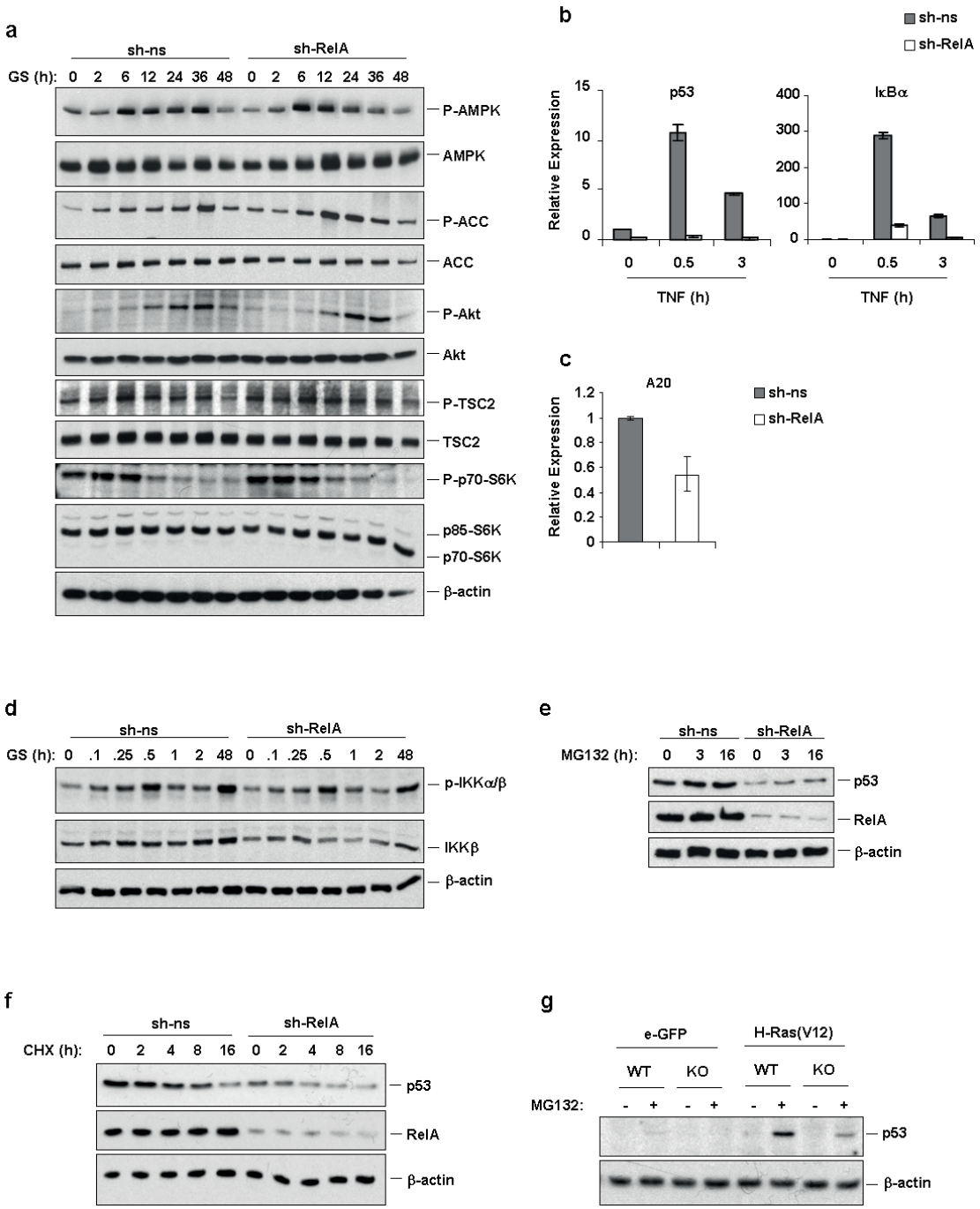

Figure S5 NF-κB upregulates p53 following TNFα stimulation or oncogenic H-Ras(V12) expression, without affecting p53 protein stability or AMPK, Akt and mTOR signalling. (**a**) Western blots showing total and phosphorylated (P) levels of upstream regulators and downstream effectors of the AMPK, Akt and mTOR pathways, controlling metabolism and nutrient uptake[1,5], in immortalized sh-ns and sh-RelA MEFs before and after GS (1 mM glucose). The proteins analyzed included: AMPK and its substrate, Acetyl CoA Carboxylase (ACC), Akt, the mTOR inhibitor, Tuberin (TSC2), and the mTOR substrate, p70-S6 Kinase (p70-S6K). (**b**) qRT-PCR with primers specific for p53 (left) or IκBα (right) and RNAs from unstimulated and TNFα-treated, immortalized MEFs expressing sh-ns or RelA-specific sh-RNAs. (**c**) qRT-PCR with primers specific for A20 and RNAs from immortalized sh-ns and sh-RelA MEFs under basal culture conditions. (**b**, **c**) Values denote mean ± s.e.m. (n=3). (**d**) Western blots with antibodies against total IκB kinase β (IKKβ) and phosphorylated (P) IKKα and IKKβ (P-IKKα/β), showing activation of the NF-κB-inducing IKK complex in immortalized MEFs expressing sh-ns or RelA-specific sh-RNAS after GS. (**e**, **f**) NF-κB does not affect p53 protein stability in cells. Western blots showing p53 and RelA expression in immortalized sh-ns and sh-RelA MEFs before and after treatment with the proteasome inhibitor, MG132 (0.5 μM) (**e**), or the protein synthesis inhibitor, cycloheximide (CHX; 10 μg/ml) (**f**). The data show that the levels of p53 proteins decrease with similar kinetics in sh-ns and sh-RelA MEFs, thus demonstrating the similar half-life of p53 in these cells. (**g**) RelA deficiency impairs the induction of p53 by oncogenic H-Ras(V12). Western blots with antibodies against p53 or β-actin and early-passage *RelA*$^{-/-}$ (KO) and wild-type (WT) MEFs expressing exogenous H-Ras(V12) or eGFP, in the presence (+) or absence (-) of MG132 (50 μM). The data show that the levels of p53 are decreased in H-Ras(V12)-expressing *RelA*$^{-/-}$ MEFs relative to H-Ras(V12)-expressing WT MEFs. (**a**, **d-g**) β-actin is shown as loading control.

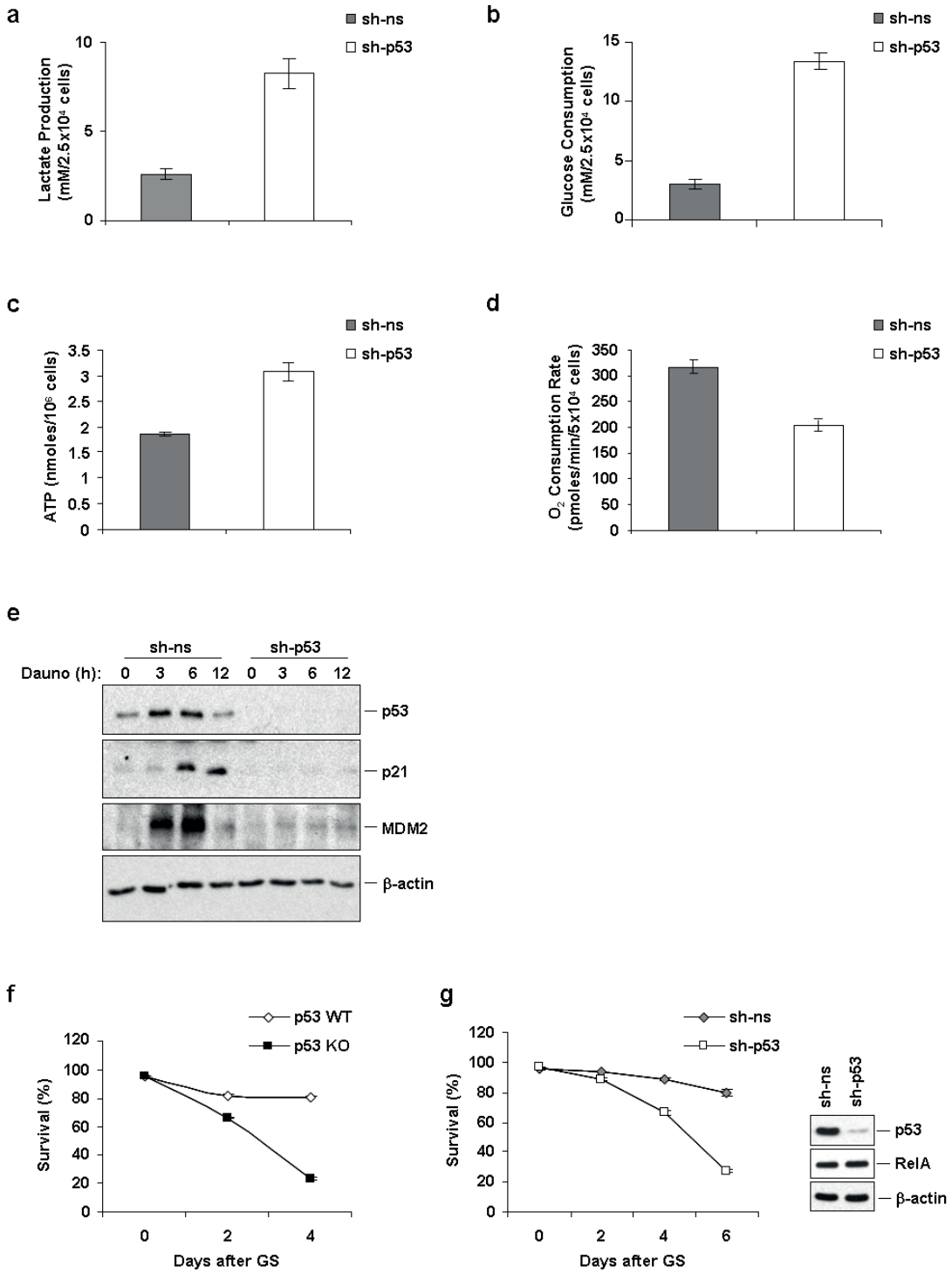

Figure S6 p53 recapitulates the effects of NF-κB on energy homeostasis and metabolic adaptation. (**a-d**) Lactate production, glucose consumption, intracellular ATP concentration, and oxygen consumption in immortalized MEFs expressing sh-ns or p53-specific sh-RNAs, under basal conditions. Similar results were obtained using an additional p53-specific sh-RNA (sh-p53-2). (**e**) Western blots with antibodies against p53 and the p53 transcriptional targets, p21 and MDM2, in immortalized MEFs expressing sh-ns or p53-specific (sh-p53) sh-RNAs before and after treatment with the DNA damaging agent, daunorubicin (Dauno). The data show that daunorubicin treatment induces a vigorous upregulation of p21 and MDM2, as well as of p53 (a target of itself), in immortalized sh-ns MEFs, but not in sh-p53 MEFs. Hence, immortalized MEFs are capable of mounting a normal p53-dependent DNA-damage response, and so contain a functional p53 pathway. (**f**, **g**) p53 promotes cell survival during GS. (**f**) Viability of early-passage *p53*$^{-/-}$ (KO) and *p53*$^{+/+}$ (WT) MEFs after GS. Similar results were obtained using two additional clones of mutant and wild-type MEFs. (**g**) Survival of sh-ns- and sh-p53-expressing immortalized MEFs after GS (left). Western blots showing p53 and RelA expression in the same MEFs (0-hour time points; right). (**e**, **g**) β-actin is shown as loading control. (**a-d**, **f**, **g**) Values denote mean ± s.e.m. (**a-c**, **f**, **g**) n=3; (**d**) n=5.

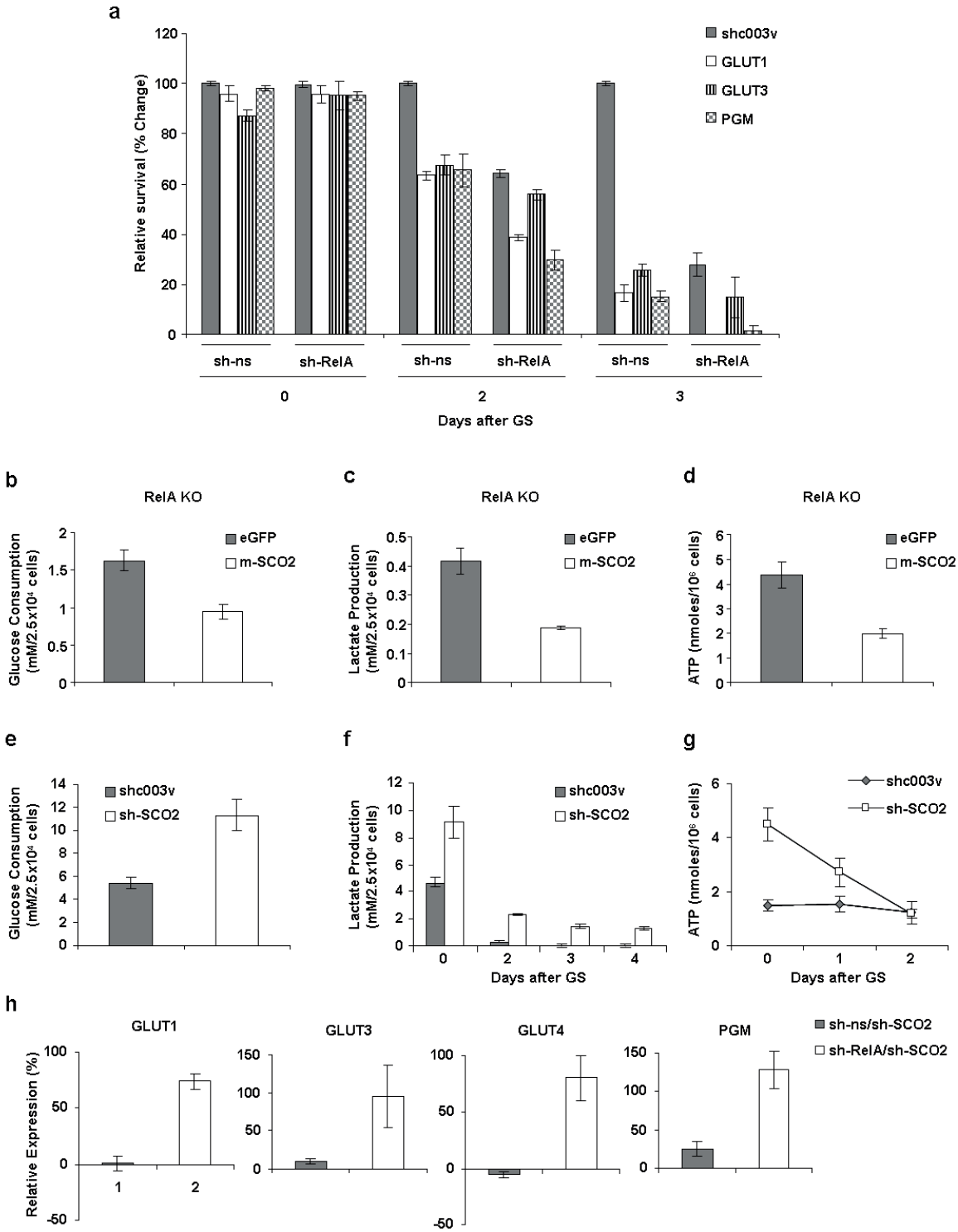

Figure S7 SCO2 mediates the metabolic activities of NF-κB. (**a**) Survival of immortalized, sh-ns and sh-RelA MEFs infected with pLKO.1-shc003v, -sh-GLUT1, -sh-GLUT3 or -sh-PGM, then subjected to GS. Values express the percentage of live cells in each culture relative to the viability observed in the respective sh-ns/shc003v control for each time point. (**b-d**) SCO2 expression reverts the metabolic effects of RelA loss. Basal glucose consumption, lactate production, and intracellular ATP concentration in early-passage *RelA*$^{-/-}$ MEFs infected with pWPT-eGFP or pWPT-SCO2. (**e-g**) SCO2 silencing mimics the metabolic effects of RelA inhibition. Glucose consumption, lactate production, and intracellular ATP concentration in immortalized MEFs expressing shc003v or SCO2-specific sh-RNAS before and/or after GS. (**h**) SCO2 silencing upregulates expression of p53 glycolytic targets in RelA-deficient, but not in wild-type cells. qRT-PCR with primers specific for GLUT1, GLUT3, GLUT4 or PGM and RNAs from immortalized, sh-ns and sh-RelA MEFs infected with either pLKO.1-shc003v (not depicted) or pLKO.1-sh-SCO2 (sh-ns/sh-SCO2 and sh-RelA/sh-SCO2, respectively). Shown is the percent change in glycolytic gene expression in sh-ns and sh-RelA cells after infection with pLKO.1-sh-SCO2 relative to expression in the respective pLKO.1-shc003v-infected controls (*see* also Fig. 3a, the basal gene expression in sh-ns and sh-RelA immortalized MEFs). (**a-h**) Values denote mean ± s.e.m. (n=3).

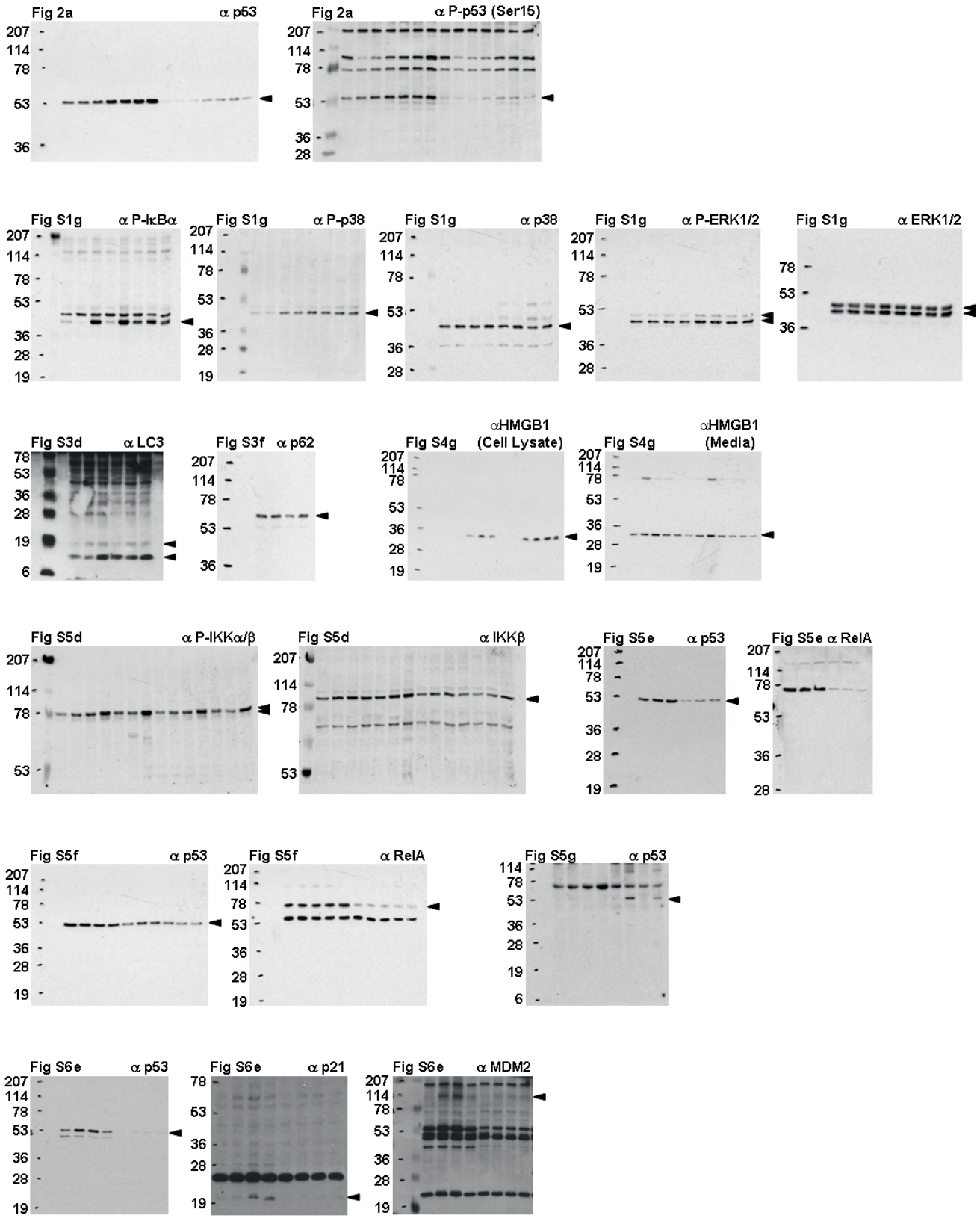

Figure S8 Full scans.